Power Engineering and Engineering Thermophysics
https://www.acadlore.com/journals/PEET

Influence of Radially Varying Magnetic Fields and Heat Sources/Sinks on MHD Free-Convection Flow Within a Vertical Concentric Annulus

Michael O. Oni*, Basant K. Jha, Junaid M. Abba, Olaife H Adebayo

Department of Mathematics, Ahmadu Bello University, 810107 Zaria, Nigeria

* Correspondence: Michael O. Oni (michaeloni29@yahoo.com)

Received: 01-25-2024 **Revised:** 03-03-2024 **Accepted:** 03-09-2024

Citation: M. O. Oni, B. K. Jha, J. M. Abba, and O. H. Adebayo, "Influence of radially varying magnetic fields and heat sources/sinks on MHD free-convection flow within a vertical concentric annulus," *Power Eng. Eng. Thermophys.*, vol. 3, no. 1, pp. 27–44, 2024. https://doi.org/10.56578/peet030103.

Abstract: In this study, an exact solution is developed to elucidate the effects of radially varying temperature-dependent heat sources/sinks (RVTDHS) and magnetic fields on natural convection flow between two vertically oriented concentric cylinders, where heating is administered through both isoflux (constant heat flux) and isothermal (constant wall temperature) conditions. The energy equation incorporates a temperature-dependent heat source/sink term, postulated to vary inversely with the radial coordinate. Through the application of suitable transformations, exact expressions for temperature distributions and fluid velocities as functions of the radial coordinate, the ratio of radii, the heat source/sink parameter, and the Hartmann number (representing magnetic field strength) are derived. Findings indicate that the presence of a radially varying heat source/sink notably influences temperature distribution, velocity profile, skin friction, and mass flux, with the heat source elevating fluid temperature. Consequently, this adjustment shortens the range over which isothermal heating supersedes isoflux heating. Conversely, in the presence of a heat sink, isothermal heating remains predominant over isoflux heating irrespective of the annular gap's size. These results not only provide deeper insights into the dynamics of magnetohydrodynamics (MHD) free-convection flows in engineering and geophysical applications but also enhance the understanding of how magnetic fields and heat sources/sinks can be strategically manipulated to control such flows.

Keywords: Radially varying heat source/sink; Free convection; Magnetohydrodynamics (MHD); Vertical annulus; Radial magnetic field

1 Introduction

The analysis of mathematical modelling and exact solutions in predicting flow formation continues to gain scientific interest owing to recent industrial applications such as cooling devices and heat transfer enhancement. Researchers have studied natural convection flow in a vertical annulus subject to isothermal or constant heat flux. For instance, El-Shaarawi and Sarhan [1] examined the dynamics of laminar flow during the development phase of natural convection within an open-ended vertical annulus, which featured a rotating inner cylinder, and employed the implicit finite difference (IFD) approach to unravel the governing boundary layer equations. It was concluded that heating at the inner cylinder had steadying properties, whereas heating at the outer cylinder had a disrupting effect. Later, Pollard and Oosthuizen [2] investigated the free convection flow through open-ended pipes. By considering two isothermal boundaries, Joshi [3] examined the fully developed free convection flows in a vertical annulus. El-Shaarawi and Sarhan [4] examined an analytical solution for developing natural convection flow in open-ended vertical concentric annuli. They used four different thermal boundary conditions and presented a closed-form solution for each case.

It is well known that some fluids are electrically conducting in nature, which has significant applications in the design of batteries and power generation. The study of such fluids continues to gain great impact owing to their promising applications. The earliest study can be found in the work of Ressow [5]. Ramamoorthy [6] inspected the flow in between two rotating concentric cylinders in the presence of a radial magnetic field. An approximate solution was obtained using the equation of motion deduced by Rossow [5]. It was inferred that the velocity was always damped in comparison to the corresponding hydrodynamic case. Later, Arora and Gupta [7] studied the MHD flow in between two coaxial rotating cylinders in the presence of a radial magnetic field. They concluded that

the behaviour exhibited by the exact solutions of the work was quite contrary to that obtained by Ramamoorthy [6]. Singh and Singh [8] proposed that the magnitude of velocity and induced magnetic field was higher in an isothermal situation in comparison to persistent heat flux.

The rising need to reduce or decrease heat transfer has increased the studies of heat generation (source) or heat absorbing (sink) fluids, which gives rise to the modelling of various mathematical formulations to predict the physical behaviour of the fluid. Inman [9] and Ostrach [10] presented a mathematical formulation for internal heat generation/absorption as a constant. While Chambre [11] and Toor [12] gave the heat source/sink as a function of space. According to Toor [13], Modejski [14] and Gee and Lyon [15], the heat source is assumed to be the expansion effects and frictional heating of the fluid. Later, Moalem [16] proposed that the basis of heat generation could be inversely related to $a + bT$. Foraboschi and Federico [17] proposed one of the most popular models. In addition, they proposed that the volumetric rate of the heat source was directly proportional to the temperature difference $(T - T_0)$. Heat generation or absorption in between two vertical concentric cylinders has been studied by several researchers [18–23].

This study is motivated by the work of Singh et al. [24] where an exact solution was presented to analyse natural convection flow in vertical concentric annuli under a radial magnetic field. It is known that the intensity of a heat source/sink increases/decreases with an increase in temperature. Hence, this study aims to develop a mathematical model for a temperature-dependent heat source or sink which is radially variable with space. This study can be viewed as a generalization of the study of Singh et al. [24] in the presence of a heat source/sink. The governing energy and momentum equations are obtained and exactly solved in closed form. Engineering interests, for example, mass flux and skin friction, are further analyzed, and the role of pertinent parameters is established graphically.

2 Mathematical Analysis

As for a steady radial flow formation in the domain $a \leq r \leq b$ of a vertical annulus filled with heatabsorbing or heat-generating fluid in the vicinity of a radial magnetic field, the radiuses of the outer and inner cylinders are denoted as b and a, respectively, as shown in Figure 1. The inner cylinder is assumed to be heated isothermally or isoflux (constant heat flux) with temperature T_w greater than the ambient temperature T_0 or at persistent rate q', whereas the outer cylinder is fixed at T_0. This unequal temperature at the walls leads to unequal density and free convection flow. A magnetic field, denoted as $\frac{B_0 a}{r}$, is focused radially outward to flow formation. It is known that this magnetic field exhibits Lorenz forces that tend to retard fluid motion. In addition, as exhibited by some fluids, the internally generated heat source or sink in the energy equation is assumed to vary radially [25]. Therefore, the heat source/sink intensity at the outer surface of the inner cylinder (the heated surface) is greater than that at the inner surface of the outer cylinder.

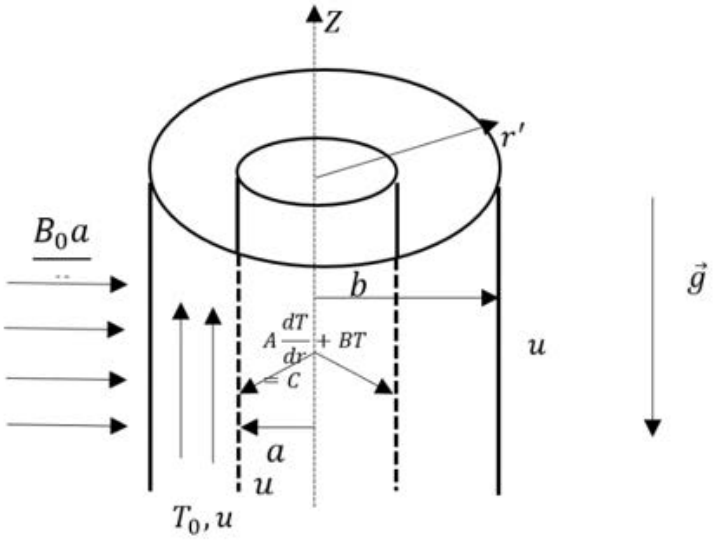

Figure 1. Schematic of the problem

These assumptions lead to the dimensionless form of the energy and momentum equations governing the flow dynamics.

$$\frac{d^2T}{dr^2} + \frac{1}{r}\frac{dT}{dr} \pm \frac{Q}{\kappa} = 0 \tag{1}$$

$$v\left[\frac{d^2u}{dr^2}+\frac{1}{r}\frac{du}{dr}\right]-\frac{\sigma {B_0}^2 a^2}{\rho r^2}u+\mathrm{g}\beta\left(T-T_0\right)=0 \tag{2}$$

They are subject to:

$$\begin{aligned} &u=0, T=T_w \quad \text{or} \quad \frac{dT}{dr}=-\frac{q}{\kappa} \quad \text{when} \quad r=a \\ &u=0, T=T_0 \text{ when } r=b \end{aligned} \tag{3}$$

where, T is the dimensional temperature, u is the dimensional velocity, κ is the thermal conductivity, v is the kinematic viscosity, σ is the electrical conductivity, μ is the dynamic viscosity, B_0 is the intensity of magnetic field, β is the coefficient of thermal expansion, g is the gravity term, and μ_e is the magnetic permeability. Q is the radially varying heat sink or source function and is defined as:

$$Q=\frac{Q_0\left(T-T_0\right)a^2}{r^2} \tag{4}$$

The following dimensionless parameters are used:

$$R=\frac{r}{a}, S=\frac{Q_0 a^2}{\kappa}, \theta=\frac{(T-T_0)}{\Delta T}, M^2=\frac{\sigma B_0^2 {\mu_e}^2 a^2}{\mu}, U=\frac{u}{u_0}, u_0=\frac{\rho g a^2 \beta\left(T_w-T_0\right)}{\mu}, \lambda=\frac{b}{a} \tag{5}$$

where, S is the heat sink/source parameter, M is the Hartmann number, θ is the dimensionless temperature, U is the dimensionless velocity, and λ is the ratio of radiuses.

2.1 Case I: Heat Sink

Considering the negative part of Eq. (1) and substituting Eq. (5) into Eqs. (2) to (4), the energy and momentum equations governing the flow formation of natural convection flow in a vertical annulus filled with temperature-dependent heat-absorbing fluid in dimensionless form are given by:

$$\frac{d^2\theta}{dR^2}+\frac{1}{R}\frac{d\theta}{dR}-\frac{S}{R^2}\theta=0 \tag{6}$$

$$\frac{d^2U}{dR^2}+\frac{1}{R}\frac{dU}{dR}-\frac{M^2}{R^2}U+\theta=0 \tag{7}$$

They are subject to:

$$\begin{aligned} &U=0, \quad A\frac{d\theta}{dR}+B\theta=C \quad \text{when} \quad R=1 \\ &U=0,\ \theta=0 \text{ or} \quad \text{when } r=\lambda \end{aligned} \tag{8}$$

where, A, B, C are constants, with $A=0, B=1, C=1$ for isothermal heating and $A=1, B=0, C=-1$ for isoflux heating.

After solving Eqs. (6) and (7) with boundary conditions (8), the following expressions are obtained for dimensionless temperature and velocity profiles, respectively:

$$\theta(R)=\frac{C\left[(R)^{-\sqrt{S}}-(R)^{\sqrt{S}}(\lambda)^{-2\sqrt{S}}\right]}{B\left(1-(\lambda)^{-2\sqrt{S}}\right)-A\sqrt{S}\left(1+(\lambda)^{-2\sqrt{S}}\right)} \tag{9}$$

$$U(R)=\frac{\left[A_3\lambda^{-M}-A_4\right]R^M+\left[A_4-A_3(\lambda)^M\right]R^{-M}}{\left[\lambda^{-M}-\lambda^M\right]}-\left[\frac{C_1(R)^{(2+\sqrt{S})}}{(2+\sqrt{S})^2-M^2}+\frac{C_2(R)^{(2-\sqrt{S})}}{(2-\sqrt{S})^2-M^2}\right] \tag{10}$$

The parameters of interest for engineering applications are the skin frictions (τ) and the mass flux of the fluid (F), which are defined in dimensionless form as:

$$\tau_1 = \left.\frac{dU}{dR}\right|_{R=1}, \quad \tau_\lambda = -\left.\frac{dU}{dR}\right|_{R=\lambda} \text{ and } \quad F = 2\pi \int_1^\lambda RU(R)dR \tag{11}$$

$$\tau_1 = M\left(C_3 - C_4\right) - 2\left[A_1(2+\sqrt{S}) + A_2(2-\sqrt{S})\right] \tag{12}$$

$$\tau_\lambda = M\left[C_4(\lambda)^{-(M+1)} - C_3(\lambda)^{M-1}\right] + \left[A_1(2+\sqrt{S})(\lambda)^{(1+\sqrt{S})} + A_2(2-\sqrt{S})(\lambda)^{(1-\sqrt{S})}\right] \tag{13}$$

$$F = 2\pi\left[\frac{C_3\left((\lambda)^{M+2}-1\right)}{(M+2)} + \frac{C_4\left((\lambda)^{2-M}-1\right)}{(2-M)} - \frac{A_1\left((\lambda)^{(4+\sqrt{S})}-1\right)}{(4+\sqrt{S})} - \frac{A_2\left((\lambda)^{(4-\sqrt{S})}-1\right)}{(4-\sqrt{S})}\right] \tag{14}$$

where,

$$C_1 = \frac{C(\lambda)^{-2\sqrt{S}}}{A\sqrt{S}\left(1+(\lambda)^{-2\sqrt{S}}\right) - B\left(1-(\lambda)^{-2\sqrt{S}}\right)}$$

$$C_2 = \frac{C}{B\left(1-(\lambda)^{-2\sqrt{S}}\right) - A\sqrt{S}\left(1+(\lambda)^{-2\sqrt{S}}\right)}$$

$$A_1 = \frac{C_1}{\left[(2+\sqrt{S})^2 - M^2\right]}$$

$$A_2 = \frac{C_1}{\left[(2-\sqrt{S})^2 - M^2\right]}$$

$$A_3 = A_1 + A_2$$

$$A_4 = A_1(\lambda)^{2+\sqrt{S}} + A_2(\lambda)^{2-\sqrt{S}}$$

$$C_3 = \frac{\left[A_3(\lambda)^{-M} - A_4\right]}{(\lambda)^{-M} - (\lambda)^{M}}$$

$$C_4 = \frac{\left[A_4 - A_3(\lambda)^{M}\right]}{(\lambda)^{-M} - (\lambda)^{M}}$$

2.2 Case II: Heat Source

When the fluid flow in the vertical annulus is assumed to be heat-generating in nature, the positive sign of Eq. (1) is considered. Following the transformation and methodology in case I, the exact solution of temperature distributions and velocity profile in dimensionless form are:

$$\theta(R) = \frac{C\left[(R)^{-i\sqrt{S}} - (R)^{i\sqrt{S}}(\lambda)^{-2i\sqrt{S}}\right]}{\left(A_6 - A_5(\lambda)^{-2i\sqrt{S}}\right)} \tag{15}$$

$$U(R) = \frac{\left[B_3\lambda^{-M} - B_4\right]R^M + \left[B_4 - B_3(\lambda)^M\right]R^{-M}}{\left[\lambda^{-M} - \lambda^M\right]} - \left[\frac{C_5(R)^{(2+\sqrt{S})}}{(2+i\sqrt{S})^2 - M^2} + \frac{C_6(R)^{(2-\sqrt{S})}}{(2-i\sqrt{S})^2 - M^2}\right] \tag{16}$$

Following a similar procedure, the expressions for skin frictions and the mass flux are given by:

$$\tau_1 = M\left(C_7 - C_8\right) - 2\left[B_1(2+i\sqrt{S}) + B_2(2-i\sqrt{S})\right] \tag{17}$$

$$\tau_\lambda = M\left[C_8(\lambda)^{-(M+1)} - C_7(\lambda)^{M-1}\right] + \left[B_1(2+i\sqrt{S})(\lambda)^{(1+i\sqrt{S})} + B_2(2-i\sqrt{S})(\lambda)^{(1-i\sqrt{S})}\right] \tag{18}$$

$$F = 2\pi\left[\frac{C_7\left((\lambda)^{M+2}-1\right)}{(M+2)} + \frac{C_8\left((\lambda)^{2-M}-1\right)}{(2-M)} - \frac{B_1\left((\lambda)^{(4+i\sqrt{S})}-1\right)}{(4+i\sqrt{S})} - \frac{B_2\left((\lambda)^{(4-i\sqrt{S})}-1\right)}{(4-i\sqrt{S})}\right] \tag{19}$$

where,

$$C_5 = \frac{C(\lambda)^{-2i\sqrt{S}}}{(Ai\sqrt{S}-B)+(B+Ai\sqrt{S})(\lambda)^{-2i\sqrt{S}}}$$

$$C_6 = \frac{C}{(Ai\sqrt{S}-B)+(B+Ai\sqrt{S})(\lambda)^{-2i\sqrt{S}}}$$

$$B_1 = \frac{C_5}{\left[(2+i\sqrt{S})^2 - M^2\right]}$$

$$B_2 = \frac{C_6}{\left[(2-i\sqrt{S})^2 - M^2\right]}$$

$$B_3 = B_1 + B_2$$

$$B_4 = B_1(\lambda)^{2+i\sqrt{S}} + B_2(\lambda)^{2-i\sqrt{S}}$$

$$C_7 = \frac{\left[B_3(\lambda)^{-M} - B_4\right]}{(\lambda)^{-M} - (\lambda)^{M}}$$

$$C_4 = \frac{\left[B_4 - B_3(\lambda)^{M}\right]}{(\lambda)^{-M} - (\lambda)^{M}}$$

3 Results and Discussion

In the findings of this investigation, an exact solution has been delineated for the formation of flow within a vertical annulus, characterized by a radially varying heat sink/source and subjected to a radially applied magnetic field. The analysis encompasses two distinct scenarios of thermal boundary conditions at the outer surface of the inner cylinder: isoflux (constant heat flux) and isothermal (constant wall temperature). The pertinent parameters governing flow formation and mass flux include the Hartmann number (M), which is directly proportional to magnetic field strength, and the heat source/sink parameter (S), which varies inversely with fluid thermal conductivity and the ratio of radiuses (λ). Throughout this analytical study, M and S have been selected over the range $0 \leq M \leq 4.0$ and $0 \leq S \leq 3.0$, respectively.

Table 1. Numerical comparison between this study and the study of Singh et al. [24] ($M = 1.5, \lambda = 2.0$)

	Singh et al. [24]				**This study S → 0**			
	Isothermal heating		Isoflux heating		Isothermal heating		Isoflux heating	
$\boldsymbol{R}$	$\theta(R)$	$U(R)$	$\theta(R)$	$U(R)$	$\theta(R)$	$U(R)$	$\theta(R)$	$U(R)$
1.0	1.0000	0.0000	0.6931	0.0000	1.0000	0.0000	0.6931	0.0000
1.1	0.8625	0.0253	0.5978	0.0176	0.8625	0.0253	0.5978	0.0176
1.2	0.7370	0.0407	0.5108	0.0282	0.7370	0.0407	0.5108	0.0282
1.3	0.6215	0.0483	0.4308	0.0335	0.6215	0.0483	0.4308	0.0335
1.4	0.5146	0.0499	0.3567	0.0346	0.5146	0.0499	0.3567	0.0346
1.5	0.4150	0.0471	0.2877	0.0326	0.4150	0.0471	0.2877	0.0326
1.6	0.3219	0.0408	0.2231	0.0283	0.3219	0.0408	0.2231	0.0283
1.7	0.2345	0.0322	0.1625	0.0223	0.2345	0.0322	0.1625	0.0223
1.8	0.1520	0.0220	0.1054	0.0153	0.1520	0.0220	0.1054	0.0153
1.9	0.0746	0.0111	0.0513	0.0077	0.0746	0.0111	0.0513	0.0077
2.0	0.000	0.0000	0.000	0.0000	0.000	0.0000	0.000	0.0000

Table 1 shows the numerical comparison, which justifies the accuracy of the presented exact solutions with those proposed by Singh et al. [24]. The evaluation provides an outstanding agreement. Table 2 and Table 3 show the

percentage changes in mass flux and skin friction in the annulus caused by adding or taking away heat for isothermal heating and isoflux heating, respectively. It is found that the percentage increases for the heat-producing fluid and decreases for the heat-absorbing fluid. In addition, this increase or decrease increases along with the increase in λ and decreases along with the increase in M. It is fascinating to find that the case of isoflux exhibits a higher response to changes in the nature of the fluid ((heat-generating or absorbing fluid) compared to the case of isothermal heating.

Table 2. Numerical values for isothermal heating with different values of λ, M and S

λ	M	S $\to$ 0		Heat Source (S=2.0)		Heat Sink (S=2.0)		Change (source) (%)		Change (sink) (%)	
		τ_1	F	τ_1	F	τ_1	F	τ_1	F	τ_1	F
	0.5	0.2684	0.1583	0.2838	0.1714	0.2551	0.1469	5.74	8.28	-10.11	-14.29
1.8	1.0	0.2633	0.1542	0.2782	0.1671	0.2502	0.1431	5.66	8.37	-10.06	-14.36
	1.5	0.2552	0.1479	0.2695	0.1603	0.2427	0.1373	5.60	8.38	-9.94	-14.35
	0.5	0.3365	0.3205	0.3647	0.3595	0.3132	0.2886	8.38	12.17	-14.12	-19.72
2.0	1.0	0.3273	0.3093	0.3546	0.3469	0.3049	0.2785	8.34	12.16	-14.02	-19.72
	1.5	0.3134	0.2922	0.3390	0.3278	0.2922	0.2631	8.17	12.18	-13.81	-19.74
	0.5	0.6840	2.9993	0.8727	4.1786	0.5688	2.2998	27.59	39.32	-34.82	-44.96
3.0	1.0	0.6360	2.7552	0.8075	3.8413	0.5311	2.1113	26.97	39.42	-34.23	-45.04
	1.5	0.5711	2.4265	0.7179	3.3868	0.4800	1.8575	25.70	39.58	-33.14	-45.15

Table 3. Numerical values for isoflux heating with different values of λ, M and S

λ	M	S $\to$ 0		Heat Source (S=2.0)		Heat Sink (S=2.0)		Change (source) (%)		Change (sink) (%)	
		τ_1	F	τ_1	F	τ_1	F	τ_1	F	τ_1	F
	0.5	0.1578	0.0930	0.2199	0.1329	0.0800	0.0252	39.35	42.90	-63.62	-81.04
1.8	1.0	0.1547	0.0907	0.2156	0.1295	0.0790	0.0248	39.37	42.78	-63.36	-80.85
	1.5	0.1500	0.0870	0.2089	0.1242	0.0775	0.0241	39.27	42.76	-62.90	-80.60
	0.5	0.2332	0.2221	0.3847	0.3792	0.1668	0.1537	64.97	70.73	-56.64	-59.47
2.0	1.0	0.2269	0.2144	0.3739	0.3659	0.1624	0.1483	64.79	70.66	-56.57	-59.47
	1.5	0.2172	0.2025	0.3576	0.3458	0.1556	0.1401	64.64	70.77	-56.49	-59.49
	0.5	0.7595	3.2950	36.033	172.530	0.3678	1.4870	4644.3	5136.1	-98.98	-99.14
3.0	1.0	0.6987	3.0269	33.343	158.610	0.3434	1.3651	4672.1	5140.0	-98.97	-99.14
	1.5	0.6275	2.6658	29.717	139.840	0.3104	1.2010	4635.7	5145.7	-98.96	-99.14

Table 4. Numerical values for isothermal heating with different values of λ, S at M = 3.0

λ	S	Heat Source			Heat Sink		
		τ_1	τ_λ	F	τ_1	τ_λ	F
	0.5	0.1779	0.0667	0.0544	0.1751	0.0648	0.0531
1.6	1.5	0.1808	0.0686	0.0558	0.1724	0.0631	0.0519
	3.0	0.1853	0.0717	0.0579	0.1686	0.0606	0.0501
	0.5	0.2232	0.0777	0.1236	0.2177	0.0743	0.1189
1.8	1.5	0.2290	0.0814	0.1287	0.2127	0.0711	0.1145
	3.0	0.2386	0.0875	0.1370	0.2056	0.0668	0.1085
	0.5	0.2624	0.0859	0.2315	0.2535	0.0806	0.2191
2.0	1.5	0.2721	0.0918	0.2452	0.2455	0.0758	0.2078
	3.0	0.2887	0.1020	0.2689	0.2346	0.0695	0.1928
	0.5	0.2965	0.0924	0.3847	0.2837	0.0849	0.3577
2.2	1.5	0.3110	0.1009	0.4155	0.2723	0.0784	0.3340
	3.0	0.3369	0.1165	0.4711	0.2573	0.0701	0.3033
	0.5	0.3989	0.1110	1.5965	0.3667	0.0934	1.3741
3.0	1.5	0.4403	0.1343	1.8893	0.3408	0.0798	1.2000
	3.0	0.5311	0.1878	2.5507	0.3102	0.0644	1.0006

Table 5. Numerical values for isoflux heating with different values of λ, S at M = 3.0

λ	S	Heat Source			Heat Sink		
		τ_1	τ_λ	F	τ_1	τ_λ	F
	0.5	0.0868	0.0325	0.0266	0.0794	0.0294	0.0241
1.6	1.5	0.0958	0.0363	0.0296	0.0731	0.0268	0.0220
	3.0	0.1133	0.0438	0.0354	0.0654	0.0235	0.0194
	0.5	0.1393	0.0485	0.0772	0.1211	0.0413	0.0661
1.8	1.5	0.1640	0.0583	0.0921	0.1071	0.0358	0.0577
	3.0	0.2233	0.0819	0.1282	0.9013	0.0297	0.0482
	0.5	0.1980	0.0648	0.1746	0.1629	0.0518	0.1407
2.0	1.5	0.2524	0.0851	0.2274	0.1384	0.0428	0.1172
	3.0	0.4294	0.1517	0.3999	0.1129	0.0334	0.0928
	0.5	0.2615	0.0815	0.3392	0.2031	0.0608	0.2561
2.2	1.5	0.3672	0.1191	0.4905	0.1660	0.0478	0.2037
	3.0	0.9347	0.3231	1.3071	0.1304	0.0355	0.1537
	0.5	0.5546	0.1543	2.2194	0.3376	0.0860	1.2648
3.0	1.5	1.5689	0.4787	6.7312	0.2429	0.0569	0.8553
	3.0	2.5676	1.4532	9.3423	0.1713	0.0356	0.5526

Table 4 and Table 5 offer the skin friction and mass flux for different values of annular gap (λ) and S for isothermal and isoflux heating, respectively. It can be observed that, for $\lambda < 2.0$ (when the annular gap is less than the radius of the inner cylinder), isothermal heating dominates skin friction at the surfaces of the cylinders and mass flux over isoflux heating in the case of a heat source. Then isoflux leads to isothermal for $\lambda \geq 2.0$ in the presence of a strongly applied heat source. This is slightly contrary to the result presented by Singh et al. [21]. The changes can be attributed to the presence of a strong heat source. For heat sink, on the other hand, isothermal heating dominates skin friction at the surfaces of the cylinders as well as mass flux for all values of λ, regardless of the heat sink intensity over isoflux heating.

In the figures in this study, the caption with "a" represents case II (heat source) while the caption with "b" represents case I (heat sink). Subgraphs (a) and (b) of Figure 2 depict the temperature distribution in the annulus for different values of S and different heating for cases II and I, respectively. It is found from subgraph (a) of Figure 2 that the temperature distribution in the annulus increases with an increase in the heat source parameter. This can be attributed to the fact that an increase in the heat source parameter leads to a corresponding increase in the amount of heat supplied to the fluid, leading to a rise in temperature distribution in the vertical annulus. In addition, the maximum temperature is obtained for the case of isoflux heating in the presence of a strong heat source parameter, which is contrary to the findings of Singh et al. [24]. This inconsistency can be attributed to the strong heat source application. On the other hand, it can be seen from subgraph (b) of Figure 2 that fluid temperature decreases with an increase in the heat sink parameter in the annulus. This can be attributed to the removal of some heating effects from the fluid. It is interesting to find that the maximum fluid temperature is obtained in the case of isothermal heating of the outer surface of the inner cylinder, regardless of the strength of the applied heat sink.

Subgraphs (a) and (b) of Figure 3 show the role of the annular gap on temperature distribution for heat and heat sink, respectively. Isothermal heating gives a larger fluid temperature and velocity than the case of isoflux when the ratio of radiuses is less than the annular gap, and vice versa [24]. However, subgraphs (a) of Figure 3 shows a contrary result. This discrepancy can be attributed to a strongly supplied heat source. For the case of heat sinks, on the other hand, subgraph (b) of Figure 3 shows that isothermal heating is always greater than isoflux heating, regardless of the annular gap.

A correspondingly similar behaviour is found for fluid velocity in subgraphs (a) and (b) of Figure 4. It is interesting to note that the inclusion of a heat source increases fluid temperature, which reduces the interval for which isothermal heating dominates isoflux heating. In a heat sink situation, isothermal heating always dominates isoflux, regardless of the annular gap.

Subgraphs (a) and (b) of Figure 5 present the corresponding role of heat-generating (source) or absorbing (sink) fluid on dimensionless velocity in the annulus for a fixed value of Hartmann number. In both cases, fluid velocities are observed to exhibit parabolic shapes. In addition, fluid velocity increases with an increase in the heat source parameter and decreases with an increase in the heat sink parameter. This can be explained by the rise/fall in temperature, which increases/reduces the kinetic energy in the fluid. In the case of heat sinks, the magnitude of fluid velocity is higher in isothermal heating compared with isoflux heating, regardless of the heat sink magnitude.

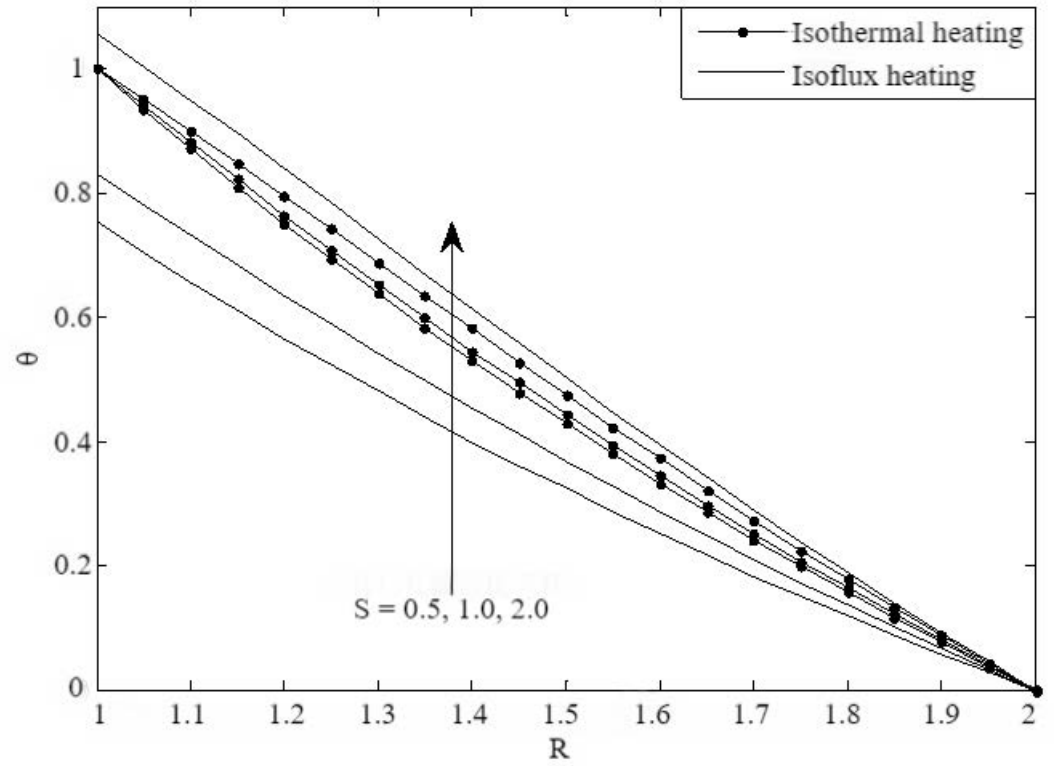

(a)

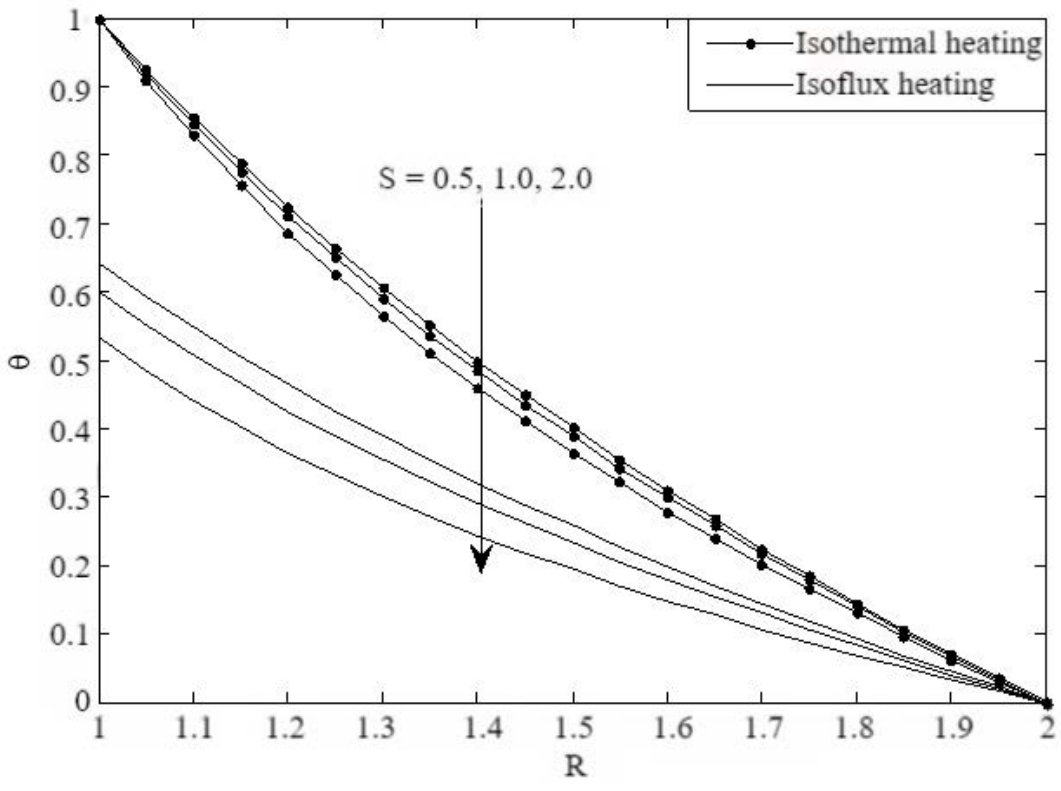

(b)

Figure 2. (a) Temperature profile for different values of S at λ=2.0 (heat source), (b) Temperature profile for different values of S and different cases at λ=2.0 (heat sink)

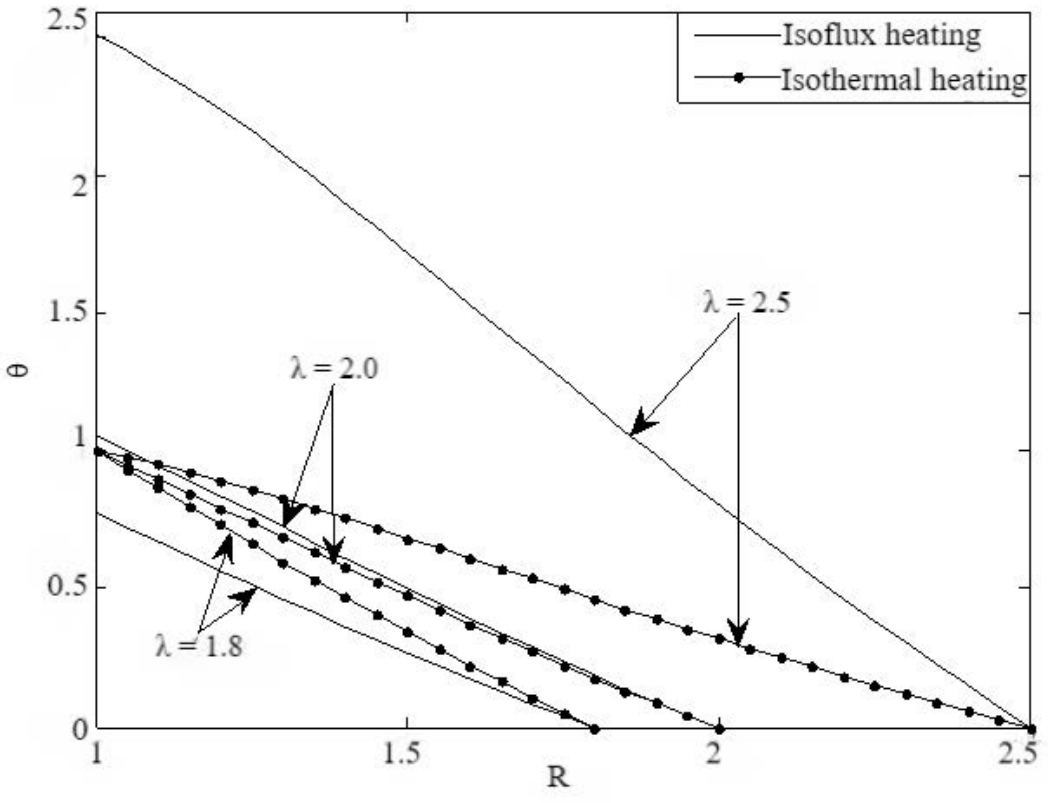

(a)

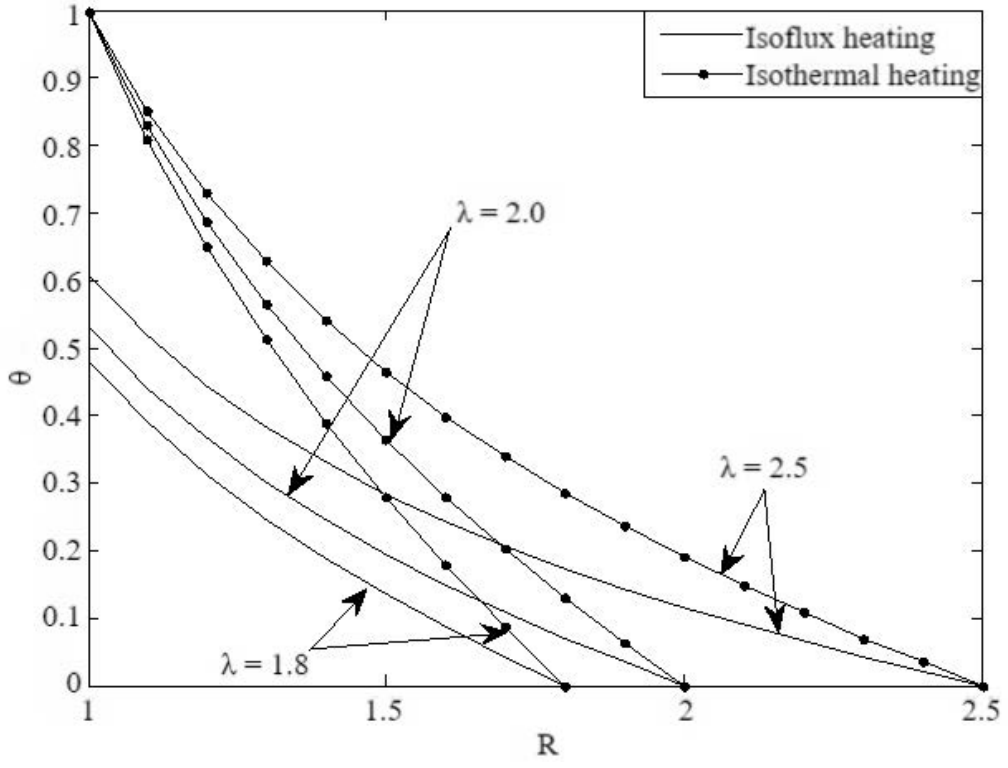

(b)

Figure 3. (a) Temperature distributions for different values of λ at M=3.0, S=2.0 (heat source), (b) Temperature Distributions for different values of λ at M=3.0, S=2.0 (heat sink)

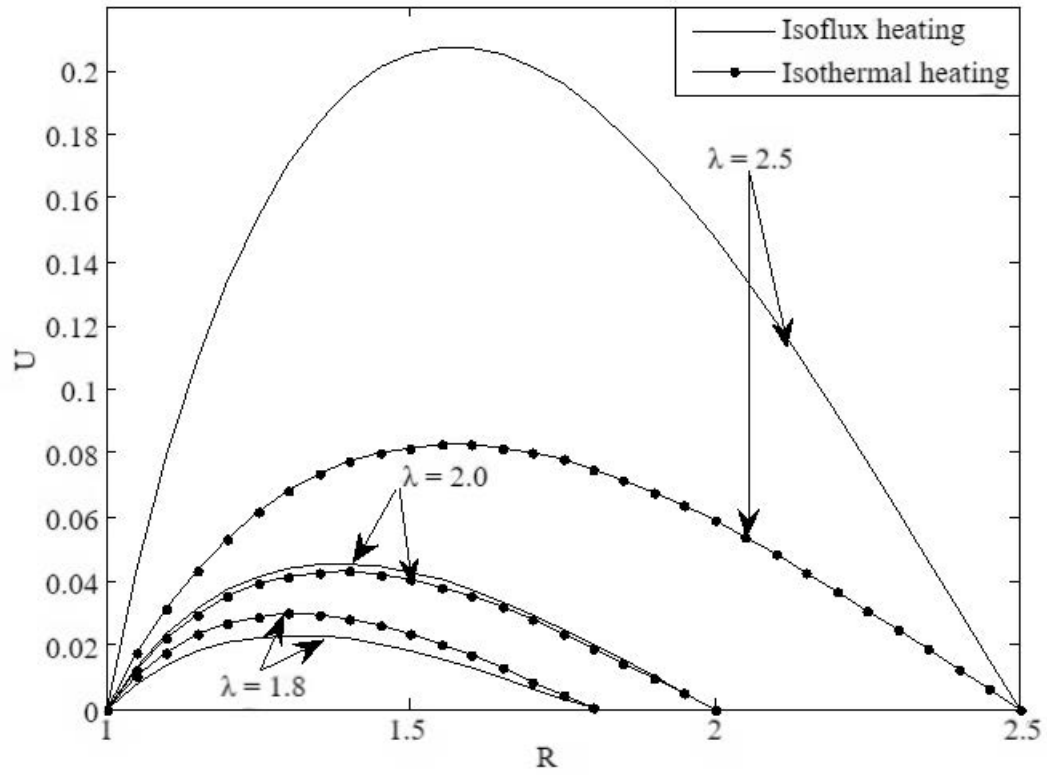

(a)

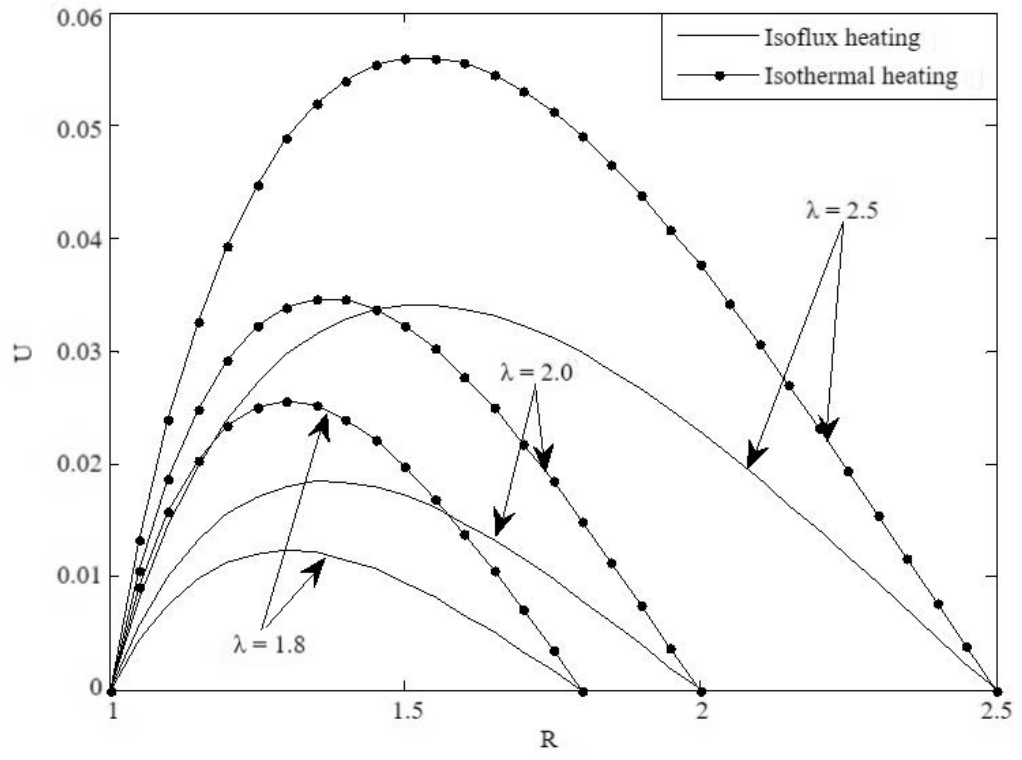

(b)

Figure 4. (a) Velocity profile for different values of λ at M=2.0, S=2.0 (heat source), (b) Velocity profile for different of λ at M=3.0, S=2.0 (heat sink)

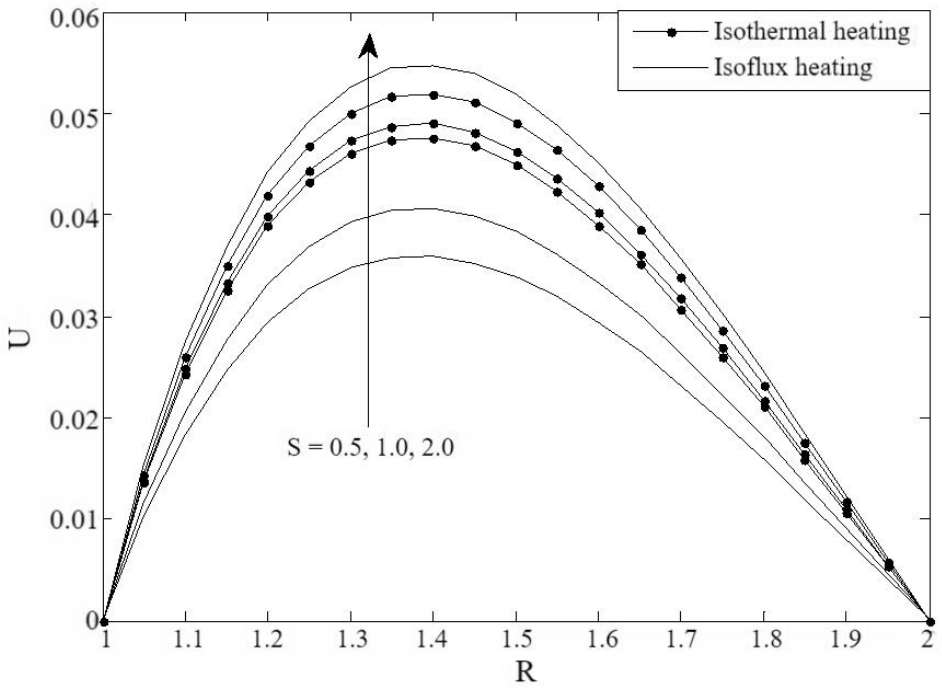

(a)

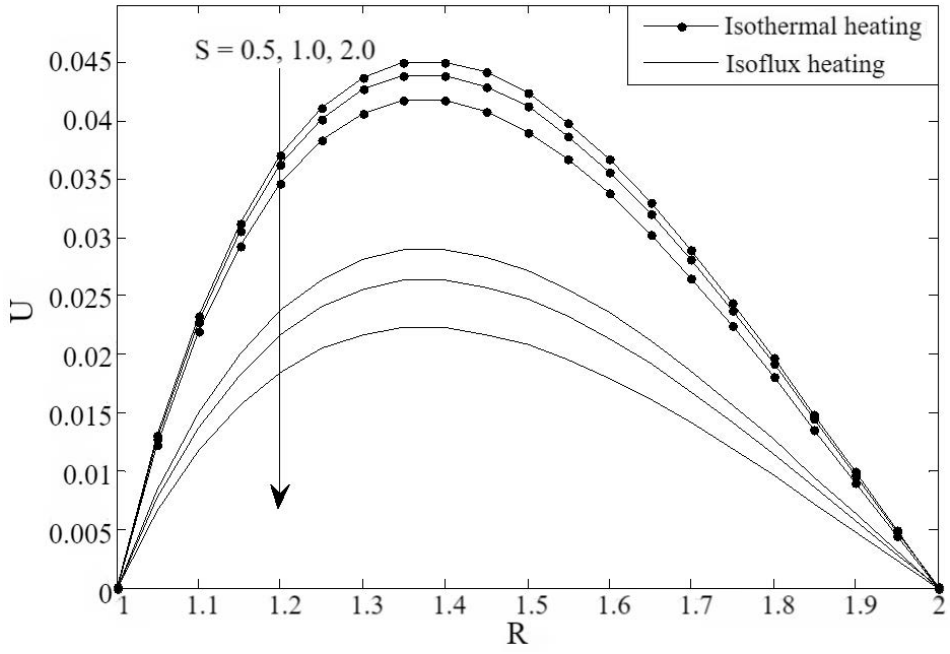

(b)

Figure 5. (a) Velocity profile for different values of S at M=2.0, λ=2.0 (heat source), (b) Velocity profile for different values of S at M=2.0, λ=2.0 (heat sink)

Subgraphs (a) and (b) of Figure 6 illustrate the role of a radially applied magnetic field on dimensionless fluid velocity for the heat source and sink, respectively, at a fixed value of the ratio of radiuses. For both cases, it is found that fluid velocity decreases with an increase in Hartmann number (M), regardless of the kind of heating considered, because the opposing Lorentz force acts in the opposite direction to the flow in the annulus. In addition, the maximum magnitude of dimensionless fluid velocity is found at the center of the annulus for the heat source (heat-generating fluid) compared with the heat-absorbing fluid. This can be explained by the fact that heat-generating fluid enhances the kinetic energy in the fluid, which increases fluid motion.

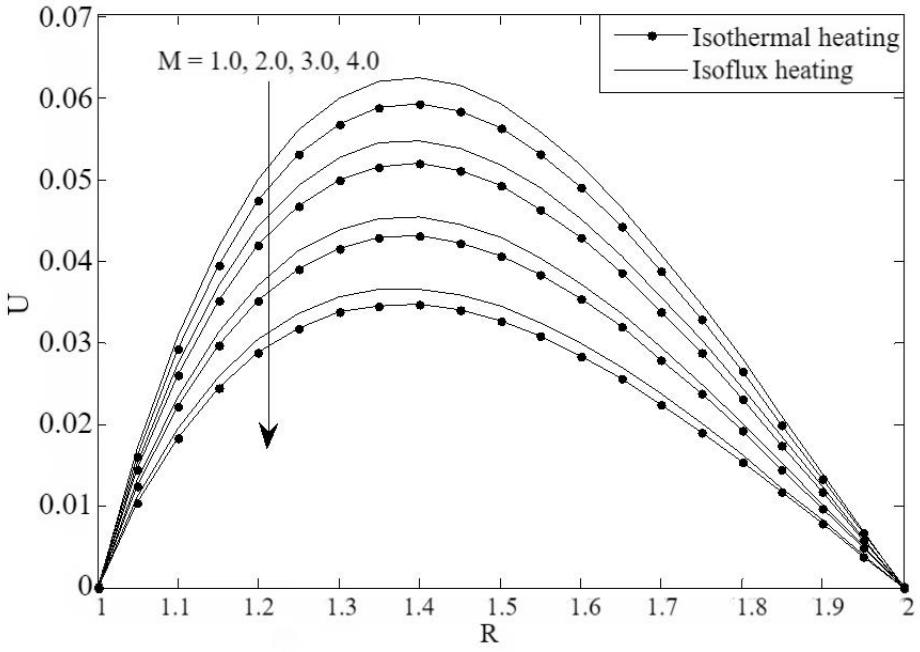

(a)

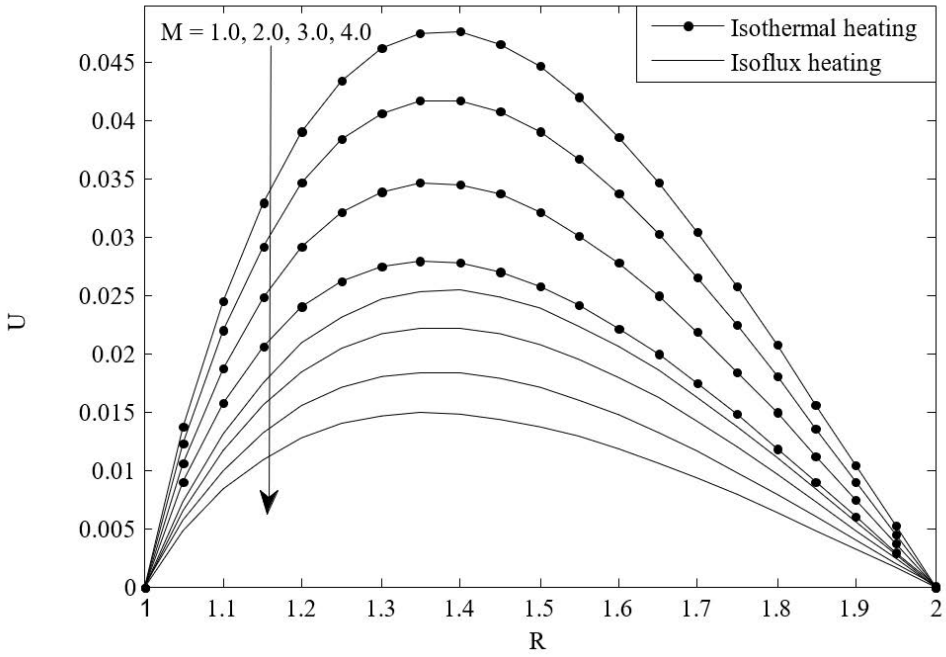

(b)

Figure 6. (a) Velocity profile for different values of M at S=2.0, λ=2.0 (heat source), (b) Velocity profile for different values of M at S=2.0, λ=2.0 (heat sink)

Subgraphs (a) and (b) of Figure 7 exhibit the role of magnetic field and heat source/sink on mass flux in the annulus for cases II and I, respectively. As shown in both figures, the mass flux decreases with an increase in magnetic field. This can be explained by the Lorenz force opposing the motion of the fluid, which decreases the amount of fluid passing through the annulus. A critical view of these figures suggests that the amount of fluid tends to zero as the magnitude of the Hartmann number tends to infinity (subgraphs (a) of Figure 6). As shown in subgraphs (a) of Figure 7, mass flux is found to increase with an increase in the heat source parameter. However, it decreases with an increase in the heat sink parameter (subgraphs (b) of Figure 7).

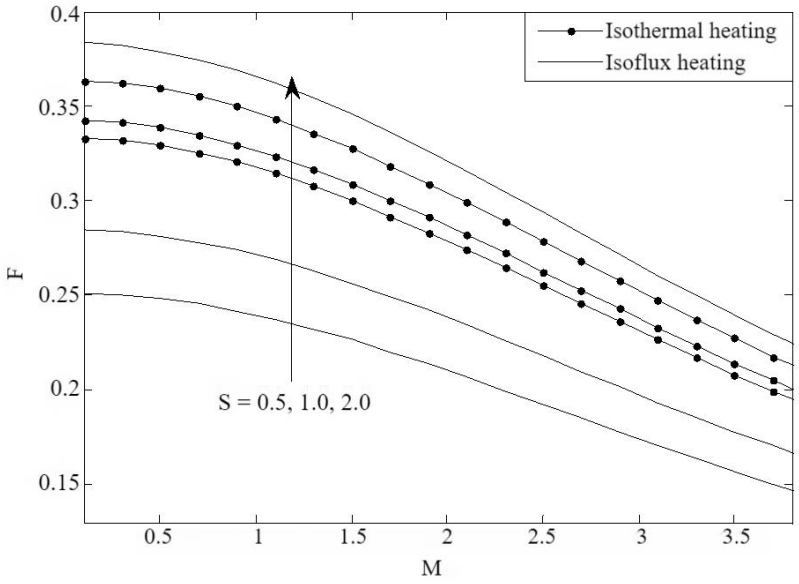

(a)

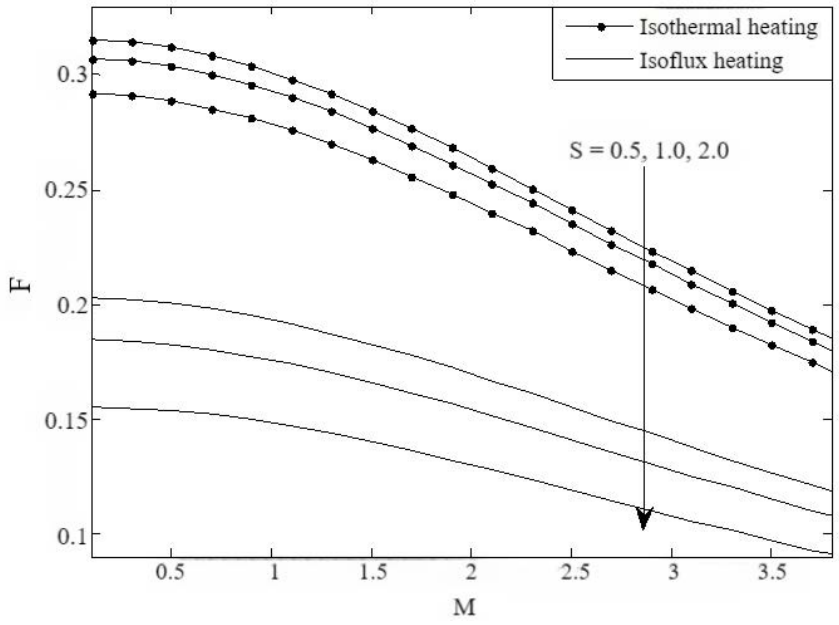

(b)

Figure 7. (a) Mass flux for different values of S and M at λ=2.0 (heat source), (b) Mass flux for different values of S and M at λ=2.0 (heat sink)

Another important analysis in fluid dynamics is to examine skin friction which is defined as the force exerted on the surfaces of the cylinders by the fluid. This notion is the basis for building dams and other fluid compressions in a cylinder.

Subgraphs (a) and (b) of Figure 8 present the combined role of a radially applied magnetic field and a radially varying heat source/sink on skin friction at the outer surface of the cylinder (the surface with isothermal or isoflux heating) for cases I and II, respectively. It is obvious from these figures that the radially applied magnetic field decreases the skin friction at this surface in both cases. This explains why the opposing Lorenz force, which decreases fluid velocity, also reduces the force at which the fluid hits the surfaces of the cylinders. The maximum skin friction can be observed when isoflux heating is considered in case II for the strong heat source parameter and $M \to 0$. On the other hand, as shown in subgraphs (b) of Figure 8, skin friction is well-behaved and highest in the case of isothermal heating than isoflux heating of the outer surface of the inner cylinder.

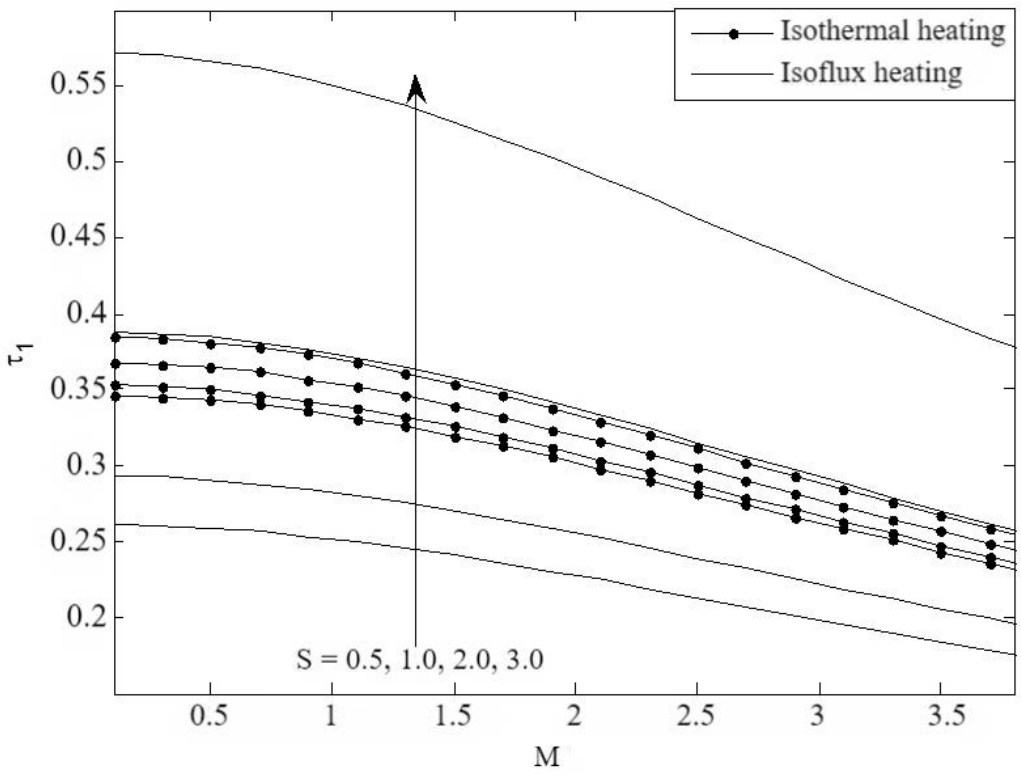

(a)

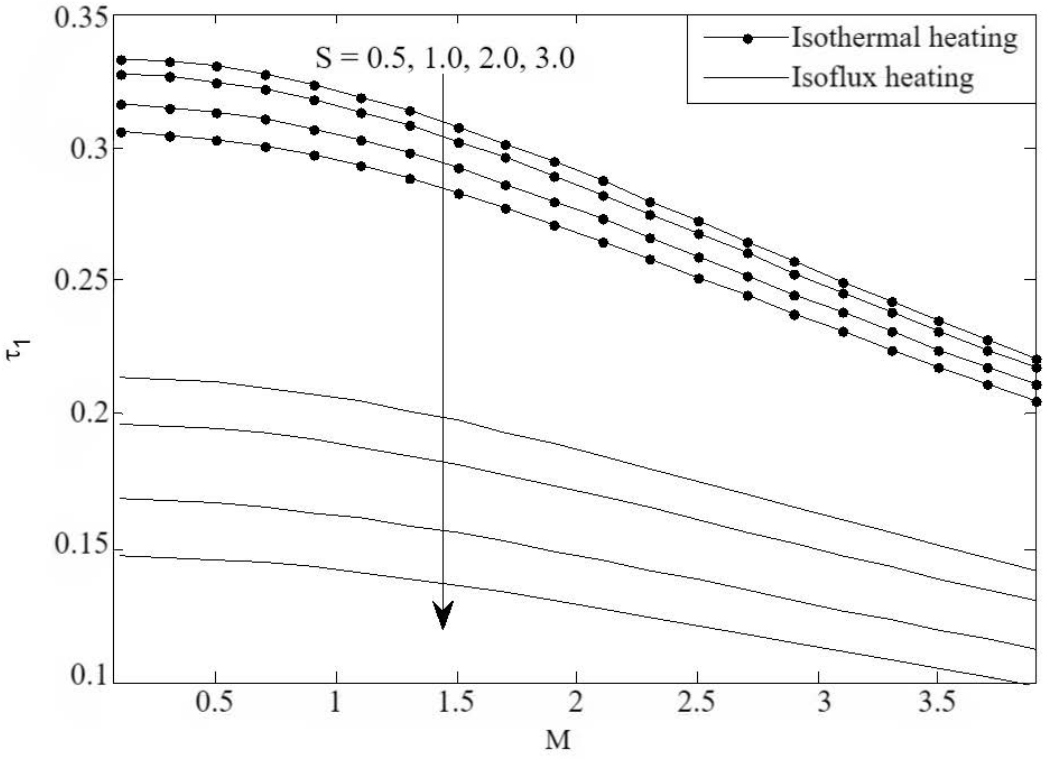

(b)

Figure 8. (a) Skin-friction for different values of S and M at λ=2.0 (R=1.0) (heat source), (b) Skin-friction for different values of S and M at λ=2.0 (R=1) (heat sink)

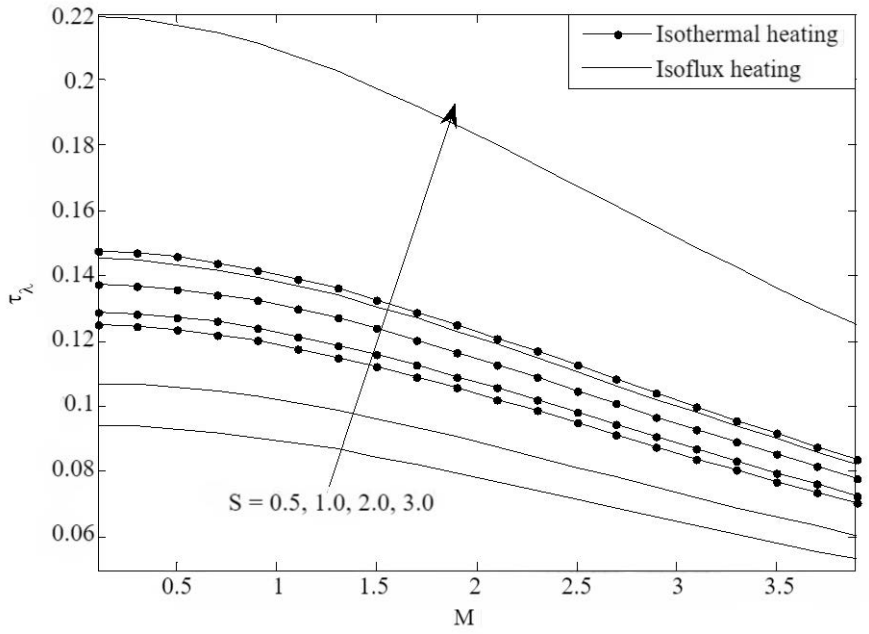

(a)

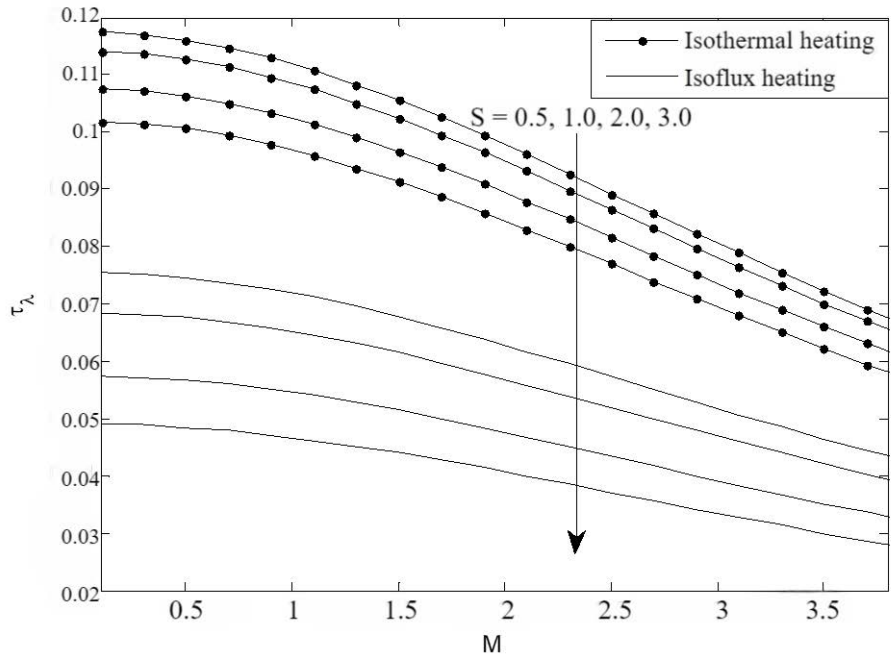

(b)

Figure 9. (a) Skin-friction for different values of S and M at λ=2.0 (R= λ) (heat source), (b) Skin-friction for different values of S and M at λ=2.0 (R=λ) (heat sink)

Subgraphs (a) and (b) of Figure 9 give the corresponding skin friction at the inner surface of the outer cylinder (the surface with ambient temperature) for cases II and I, respectively. These figures exhibit similar patterns to those in Subgraphs (a) and (b) of Figure 8. It is interesting to find that the maximum skin friction is observed at the outer surface of the inner cylinder. This can be attributed to the fact that the temperature at this surface is greater than the ambient fluid temperature exhibited by the inner surface of the outer cylinder. Figure 10 depicts the mass flow rate for different values of M and S. It is found from this figure that flowrate decreases with increase in Harmann number but increases with suction parameter at the outer cylinder. Figure 11 illustrates that skin friction reduces continually with a strongly applied magnetic field. This finding suggests that a way of reducing skin friction is to lower the temperature at the considered wall and apply a strong magnetic field.

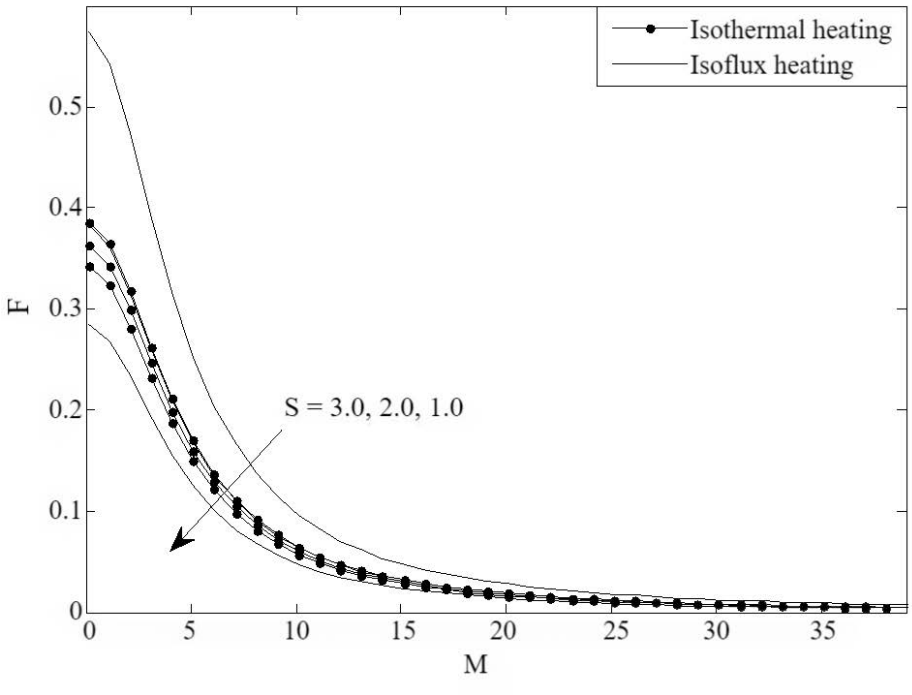

Figure 10. Mass flux for different values of M and S at λ=2.0

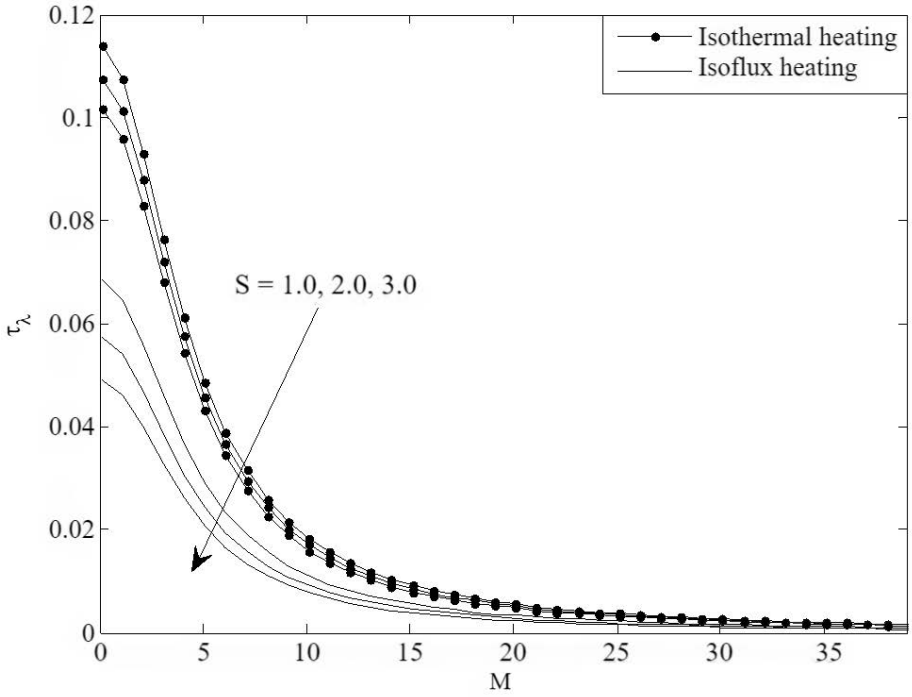

Figure 11. Skin-friction for different values of M and S at λ=2.0 (heat sink)

4 Conclusion

This study presents an exact solution to investigate the role of radially varying heat-generating or absorbing fluid in a vertical annulus subjected to isothermal or isoflux heating. The major conclusions are presented as follows:

- The increase in heat source increases fluid temperature, velocity, skin friction and mass flux. However, the reverse occurs for heat sinks.
- The implementation of a radially applied magnetic field retards flow formation, skin friction, and mass flux, regardless of the nature of the fluid or heating.

- The isothermal heating gives a higher magnitude of temperature, velocity, skin friction and mass flux for $\lambda \leq 2.0$. Then isoflux dominates for $\lambda > 2.0$ in the absence of a heat source, while the reverse occurs in the presence of a strongly applied heat source.
- Due to a radially applied magnetic field, the percentage increase or decrease in skin friction and mass flux increases with an increase in the ratio of radiuses and decreases with the Hartmann number.

Data Availability

The data used to support the findings of this study are available from the corresponding author upon request.

Conflicts of Interest

The authors declare no conflict of interest.

References

[1] M. A. I. El-Shaarawi and A. Sarhan, "Developing laminar free convection in an open ended vertical annulus with a rotating inner cylinder," *ASME J. Heat Transf.*, vol. 103, no. 3, pp. 552–558, 1981. https://doi.org/10.1115/1.3244501

[2] A. Pollard and P. Oosthuizen, "Free convection through open-ended pipes," *ASME*, vol. 105, no. 10, pp. 93–93, 1983.

[3] H. M. Joshi, "Fully developed natural convection in an isothermal vertical annular duct," *Int. Commun. Heat Mass Transf.*, vol. 14, no. 6, pp. 657–664, 1987. https://doi.org/10.1016/0735-1933(87)90045-5

[4] M. A. I. El-Shaarawi and M. A. Al-Nimr, "Fully developed laminar natural convection in open-ended vertical concentric annuli," *Int. J. Heat Mass Transf.*, vol. 33, no. 9, pp. 1873–1884, 1990. https://doi.org/10.1016/0017-9310(90)90219-K

[5] V. J. Rossow, "On flow of electrically conducting fluids over a flat plate in the presence of a transverse magnetic field," *NACA-TN*, no. NACA-TR-1358, 1958.

[6] P. Ramamoorthy, "Flow between two concentric rotating cylinders with a radial magnetic field," *Phys. Fluids*, vol. 4, no. 11, 1961. https://doi.org/10.1063/1.1706237

[7] K. L. Arora and P. R. Gupta, "Magnetohydrodynamic flow between two rotating coaxial cylinders under radial magnetic field," *Phys. Fluid*, vol. 15, no. 6, pp. 1146–1148, 1972. https://doi.org/10.1063/1.1694041

[8] R. K. Singh and A. K. Singh, "Effect of induced magnetic field on natural convection in vertical concentric annuli," *Acta Mech. Sin.*, vol. 28, pp. 315–323, 2012. https://doi.org/10.1007/s10409-012-0052-4

[9] R. M. Inman, "Experimental study of temperature distribution in laminar tube flow of a fluid with internal heat generation," *Int. J. Heat Mass Transf.*, vol. 5, no. 11, pp. 1053–1058, 1962. https://doi.org/10.1016/0017-9310(62)90058-3

[10] S. Ostrach, "Combined natural- and forced-convectionflow and heat transfer of fluids with and without heat sources in channels with linearly varying wall temperatures," National Advisory Committee for Aeronautics, Tech. Rep. NACA-TN-3141, 1954.

[11] P. L. Chambré, "The laminar boundary layer with distributed heat sources or sinks*," *Appl. Sci. Res., Sect. A*, vol. 6, no. 5, pp. 393–401, 1957. https://doi.org/10.1007/BF03185044

[12] H. L. Toor, "Heat transfer in forced convection with internal heat generation," *AIChE J.*, vol. 4, no. 3, pp. 319–323, 1958. https://doi.org/10.1002/aic.690040317

[13] H. L. Toor, "The energy equation for viscous flow-effect of expansion on temperature profiles," *Ind. Eng. Chem.*, vol. 48, no. 5, pp. 922–926, 1956. https://doi.org/10.1021/ie50557a035

[14] J. Madejski, "Temperature distribution in channel flow with friction," *Int. J. Heat Mass Transf.*, vol. 6, no. 1, pp. 49–51, 1963. https://doi.org/10.1016/0017-9310(63)90028-0

[15] R. E. Gee and J. B. Lyon, "Non isothermal flow of viscous non-newtonian fluids," *Ind. Eng. Chem.*, vol. 49, no. 6, pp. 956–960, 1957. https://doi.org/10.1021/ie50570a024

[16] D. Moalem, "Steady state heat transfer within porous medium with temperature dependent heat generation," *Int. J. Heat Mass Transf.*, vol. 19, no. 5, pp. 529–537, 1976. https://doi.org/10.1016/0017-9310(76)90166-6

[17] F. P. Foraboschi and I. Di Federico, "Heat transfer in laminar flow of non-newtonian heat-generating fluids," *Int. J. Heat Mass Transf.*, vol. 7, no. 3, pp. 315–325, 1964. https://doi.org/10.1016/0017-9310(64)90107-3

[18] B. K. Jha and A. O. Ajibade, "Free convective flow of heat generating/absorbing fluid between vertical porous plates with periodic heat input," *Int. Commun. Heat Mass Transf.*, vol. 36, no. 6, pp. 624–631, 2009. https://doi.org/10.1016/j.icheatmasstransfer.2009.03.003

[19] M. O. Oni, "Combined effect of heat source, porosity and thermal radiation on mixed convection flow in a vertical annulus: An exact solution," *Eng. Sci. Technol., Int. J.*, vol. 20, no. 2, pp. 518–527, 2017. https://doi.org/10.1016/j.jestch.2016.12.009

[20] B. K. Jha, M. O. Oni, and B. Aina, "Steady fully developed mixed convection flow in a vertical micro-concentric-annulus with heat generating/absorbing fluid: An exact solution," *Ain Shams Eng. J.*, vol. 9, no. 4, pp. 1289–1301, 2018. https://doi.org/10.1016/j.asej.2016.08.005

[21] M. Sheikholeslami, D. D. Ganji, H. R. Ashorynejad, and H. B. Rokni, "Analytical investigation of Jeffery-Hamel flow with high magnetic field and nanoparticle by adomian decomposition method," *Appl. Math. Mech.*, vol. 33, pp. 25–36, 2012. https://doi.org/10.1007/s10483-012-1531-7

[22] H. Guo, P. Lin, and L. Li, "Asymptotic solutions for the asymmetric flow in a channel with porous retractable walls under a transverse magnetic field," *Appl. Math. Mech.*, vol. 39, no. 8, pp. 1147–1164, 2018. https://doi.org/10.1007/s10483-018-2355-6

[23] F. M. Ali, R. Nazar, N. M. Arifin, and I. Pop, "MHD stagnation-point flow and heat transfer towards stretching sheet with induced magnetic field," *Appl. Math. Mech.*, vol. 32, no. 4, pp. 409–418, 2011. https://doi.org/10.1007/s10483-011-1426-6

[24] S. K. Singh, B. K. Jha, and A. K. Singh, "Natural convection flow in a vertical concentric annuli under a radial magnetic field," *Heat Mass Transfer*, vol. 32, pp. 399–401, 1997. https://doi.org/10.1007/s002310050137

[25] C. Y. Chow, *An Introduction to Computational Fluid Mechanics*. New York: John Wiley & Sons, 1979.